Korean J. Chem. Eng., **27**(1), 37-44 (2010)
DOI: 10.1007/s11814-010-0102-1

Sensitivity of spinning process with flow-induced crystallization kinetics using frequency response method

Jang Ho Yun*, Dong Myeong Shin, Joo Sung Lee***, Hyun Wook Jung*,†, and Jae Chun Hyun***

*Department of Chemical and Biological Engineering, Korea University, Seoul 136-713, Korea
**Cheil Industries Display Material Research Institute, Uiwang 437-711, Korea
***LG Chem Research Park, Daejeon 305-380, Korea
(*Received 24 August 2009 • accepted 2 November 2009*)

Abstract−The sensitivity of the low- and high-speed spinning processes incorporated with flow-induced crystallization has been investigated using frequency response method, based on process conditions employed in Lee et al. [1] and Shin et al. [2,3]. Crystallinity occurring in the spinline makes the spinning system less sensitive to any disturbances when it has not reached its maximum onto the spinline in comparison with the spinning case without crystallization. Whereas, the maximum crystallinity increases the system sensitivity to disturbances, interestingly exhibiting high amplitude value of the spinline area at the take-up in low frequency regime. It also turns out that neck-like deformation in the spinline under the high-speed spinning conditions plays a key role in determining the sensitivity of the spinning system.

Key words: Flow-induced Crystallization, Fiber Spinning, Draw Resonance, Frequency Response Method, Sensitivity, Neck-like Deformation

INTRODUCTION

The fiber spinning process, as in the other polymer extensional deformation processes such as film casting and film blowing, can be susceptibly affected by unexpected disturbances which cause the non-uniformity of fiber products. Accordingly, many researchers in academia and industry have explored the stability and sensitivity issues in this process for the enhanced control of product quality and processability during the past four decades [4-12]. Stability studies have mainly focused on the draw resonance phenomenon which is distinguished by the self-sustained periodic oscillation of spinline variables like spinline cross-sectional area and spinline tension over the critical onsets. From the linear stability analysis and direct transient simulation, stability windows for various fluids have been established in spinning systems [13-20]. Recently, Yun et al. [20] revisited the limit cycles of draw resonance using Hopf bifurcation theory, reporting that draw resonance is a supercritical Hopf bifurcation by directly calculating limit cycles and eigenvalues of monodromy matrix over one period of oscillation.

Sensitivity analysis can also provide the essential information on the dynamic of polymer processes since this straightforwardly influences the uniformity of products. Since the first reports on the sensitivity study for polymer extensional deformation processes [6,7], the sensitivity in this process has been extensively exploited, especially using frequency response method, which measures amplitudes of state variables with respect to ongoing sinusoidal disturbances in the linearized systems [8, 17-19,21,22]. Also, from the nonlinear transient simulations, Jung et al. [13] and Lee et al. [16] elucidated the role of tension sensitivity to stabilize the spinning system. McHugh group extended the frequency response method to explain the effect of crystallization kinetics using their two-phase fluid model on the sensitivity of spinning under the conditions with not fully developed crystallinity in the spinline [21,22].

In this paper, the effect of the spinline crystallinity on the sensitivity in spinning process incorporated with one-phase crystallization kinetics has been revamped using the frequency response method in both low-speed and high-speed spinning cases. Flow models and process conditions to further carry out the sensitivity analysis are based on Lee et al. [1] in low-speed spinning case and Shin et al. [2,3] in high-speed spinning case, respectively, which only inspected stability or draw resonance issues. It is noted here that the neck-like deformation in spinline under the high-speed conditions, one of the fascinating nonlinear phenomena in spinning processes, is closely related to the flow-induced crystallization. It has been revealed that the spinline crystallinity contrarily affects the spinning sensitivity whether it is fully developed in the spinline or not.

GOVERNING EQUATIONS FOR SPINNING FLOWS

To numerically compute the spinning system, as employed in the precedent stability studies [1-3], one-dimensional (1-D) flow coordinate was adopted disregarding radial variation of state variables because the spinning is totally governed by uniaxial extensional flow (Fig. 1). As eloquently introduced in Ziabicki [23] and Ziabicki and Kawai [24], secondary forces such as inertia, gravity, air drag were of course included in equation of motion. Phan-Thien and Tanner (PTT) constitutive equation which can quantitatively portray extensional behavior and ensure mathematical stability was

†To whom correspondence should be addressed.
E-mail: hwjung@grtrkr.korea.ac.kr
‡This paper is dedicated to Professor Jae Chun Hyun for celebrating his retirement from Department of Chemical and Biological Engineering of Korea University.

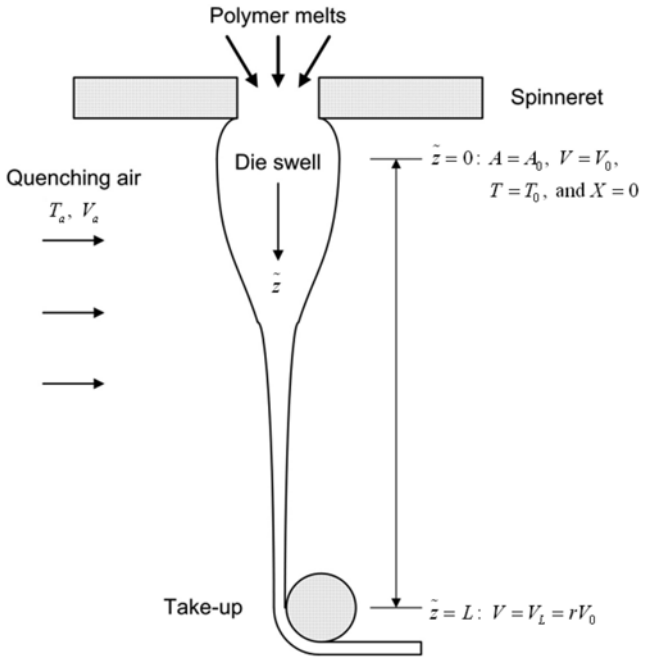

Fig. 1. Schematic diagram of melt spinning process.

involved as a viscoelastic fluid model [25]. A one-phase crystallization model was selected for predicting the crystallization kinetics in spinline [1-3,10-12]. Dimensionless governing equations for fiber spinning process are expressed as follows.

Equation of continuity:

$$\frac{\partial a}{\partial t}+\frac{\partial (av)}{\partial z}=0 \tag{1}$$

where, $a=\frac{A}{A_0}$, $v=\frac{V}{V_0}$, $t=\frac{\tilde{t}}{L/V_0}$, $z=\frac{\tilde{z}}{L}$

Equation of motion:

$$C_{in}\left(\frac{\partial v}{\partial t}+v\frac{\partial v}{\partial z}\right)=\frac{1}{a}\frac{\partial (a\tau)}{\partial z}+C_{gr}-C_{ad}v^{1.19}a^{-0.905} \tag{2}$$

where, $\tau=\frac{\tilde{\tau}}{2\eta_0 V_0/L}$, $C_{in}=\frac{\rho V_0 L}{2\eta_0}$, $C_{gr}=\frac{\rho g L^2}{2\eta_0 V_0}$,

$$C_{ad}=\frac{3.122\times10^{-4}V_0^{0.19}L^2}{2A_0^{0.905}\eta_0}$$

Constitutive equation (PTT model):

$$K\tau+De\left[\frac{\partial \tau}{\partial t}+v\frac{\partial \tau}{\partial z}-2(1-\xi)\tau\frac{\partial v}{\partial z}\right]=\frac{\eta}{\eta_0}\frac{\partial v}{\partial z} \tag{3}$$

where, $K=\exp\left[\frac{2\varepsilon De_0\tau}{\exp(3.2x)}\right]$, $\eta=\eta_0\exp\left[\frac{E}{RT_0}\left(\frac{1}{\theta}-1\right)+\alpha^* x\right]$,

$$De=De_0\exp\left[\frac{E}{RT_0}\left(\frac{1}{\theta}-1\right)+(\alpha^*-3.2)x\right],\ De_0=\frac{\lambda_0 V_0}{L}$$

Energy equation:

$$\frac{\partial \theta}{\partial t}+v\frac{\partial \theta}{\partial z}=-Stv^{1/3}a^{-5/6}(\theta-\theta_a)\left[1+64\left(\frac{v_a}{v}\right)^2\right]^{1/6}+\Delta H_f\left(\frac{\partial x}{\partial t}+v\frac{\partial x}{\partial z}\right) \tag{4}$$

where, $St=\frac{1.67\times10^{-4}L}{\rho C_p V_0^{2/3}A_0^{5/6}}$, $\theta=\frac{T}{T_0}$, $\theta_a=\frac{T_a}{T_0}$, $v_a=\frac{V_a}{V_0}$,

$$\Delta H_f=\frac{\Delta H_f^* X_\infty}{C_p T_0}$$

Crystallinity equation:

$$\frac{\partial x}{\partial t}+v\frac{\partial x}{\partial z}=n\left[\ln\left(\frac{1}{1-x}\right)\right]^{(n-1)/n}$$
$$\times(1-x)k_m\exp\left[-4\ln 2\left(\frac{\theta-\theta_m}{d}\right)^2+2\kappa\tau De_0\right] \tag{5}$$

where, $x=\frac{X}{X_\infty}$, $k_m=\frac{K_{max}L}{V_0}$, $\theta_m=\frac{T_{max}}{T_0}$, $d=\frac{D}{T_0}$

Boundary conditions:

v=1, a=1, θ=1, x=0 at z=0

v=r at z=1 (6)

where, a, v, t, z denote the dimensionless spinline cross-sectional area, spinline velocity, time, distance in the flow direction, respectively, and τ the axial stress, ρ the fluid density, V_0 the extrusion velocity, L the spinline distance, η_0 the zero shear viscosity, η the shear viscosity, g the gravity acceleration constant. C_{in} denotes the inertia coefficient, C_{gr} the gravity coefficient, C_{ad} the air drag coefficient, ε and ξ represent the PTT model parameters, λ the relaxation time, De the Deborah number, St the Stanton number, θ the dimensionless spinline temperature, x the dimensionless crystallinity. E indicates the activation energy, R the gas constant, α^* the model parameter representing the crystallinity dependency of the viscosity, V_a the cooling air velocity, T_a the cooling air temperature, T_0 the extrusion temperature, C_p, ΔH_f, X, K_{max}, T_{max}, D, κ the heat capacity, crystallization heat, maximum crystallinity, maximum crystallization

Table 1. Material properties of iPP for low-speed spinning process and Nylon-6,6 for high-speed spinning process

Material properties	iPP for low speed	Nylon-66 for high speed
Density, ρ (kg/m^3)[a]	[e]970	[f]1000
Heat capacity, C_p (J/gK)	[e]1.926	[f]2.553
Zero-shear viscosity, η_0 (Pa·s)	[e]3420	[h]1454.8
Relaxation time, λ_0 (s)	[e]0.04	[f]0.001
PTT model parameters, ε & ξ	[h]0.015, 0.6	[h]0.015, 0.35
Activation energy, E/R (K)	[e]5602	[f]6600
Heat of crystallization, ΔH_f^* (J/g)	[e]148.453	[f]188.406
Maximum crystallization rate, k_m (s^{-1})	[a]0.55	[g]1.64
Temperature at max. crystallization rate, T_{max} (K)	[a]338	[g]423
Crystallization half width temperature range, D (K)	[a]333	[g]313
Maximum crystallinity, X_∞ (%)	[c]55	[f]45
Crystallinity dependency parameter of viscosity, α^*	[d]5.1	[h]5.1
Flow-induced crystallization enhancement factor, κ	[c]8.2	[h]0.9

[a]Ziabicki, 1976 [23]
[b]Minoshima et al., 1980 [31]
[c]Kolb et al., 2000 [27]
[d]Muslet and Kamal, 2004 [26]
[e]Zheng and Kennedy, 2004 [32]
[f]Joo et al., 2002 [12]
[g]Ziabicki and Kawai, 1985 [24]
[h]Shin et al., 2006 [3]

Table 2. Process conditions of iPP for low-speed spinning process and Nylon-6,6 for high-speed spinning process

Extrusion velocity, V_0 (m/s)	Low speed	0.01
	High speed	0.5
Drawdown ratio, $r=V_0/V_r$		Changeable
Quenching air velocity, V_a (m/s)		0
Temperature at spinneret, T_0 (K)	Low speed	483
	High speed	553
Quenching air temperature, T_a (K)		298
Spinline, L (m)		1
Spinneret diameter (m)		0.00065, 0.00045

rate, temperature at maximum crystallization rate, crystallization half width temperature range, and FIC enhancement factor, respectively. n, Avrami index, is set to unity in the uniaxial extension flow. Finally, r is drawdown ratio.

The fluid viscosity and the relaxation time are functions of both temperature and crystallinity, preventing an abnormal accretion of the spinline stress, whereas the fluid modulus is mainly dependent on the crystallinity [26]. The trace of extra tensor in the flow-induced term of the crystallinity equation is simply reduced to the single axial extra stress, τ, in our 1-D model [2,3].

The sensitivity of fiber spinning has been separately analyzed here for low-speed and high-speed systems, depending on the extrusion velocity condition. In low-speed spinning case, inertia term is negligible due to low Reynolds number, whereas, in high-speed spinning case, it remarkably plays a key role in making neck-like deformation. In this study, two different material and operating conditions have been taken in low- and high-speed spinning cases from Lee et al. [1] and Shin et al. [2,3], respectively, which concentrated on draw resonance stability. For instance, isotactic polypropylene (iPP) known as a well-crystallizable polymer in the literature [27] has been considered in low-speed case and for the high-speed spinning system, Nylon-6,6 has been adopted based on Haberkorn's experimental data [3,28]. Material properties and process conditions used in each system are listed in Tables 1 and 2.

FREQUENCY RESPONSE METHOD

Sensitivity of the system to disturbances is conventionally examined by frequency response method, measuring sinusoidal output of the linearized system subjected to tiny outgoing sinusoidal inputs or disturbances. Most information about the linear dynamical behavior, including the amplitude or gain, and the phase angle in Bode plots, can be interpreted from this analysis. The sustained oscillatory perturbations can be imposed in the following spinline variables.

$$\begin{aligned}
&\text{Area} && : a(z,t)=a_s(z)+\alpha(z)\exp(i\omega t)\\
&\text{Velocity} && : v(z,t)=v_s(z)+\beta(z)\exp(i\omega t)\\
&\text{Stress} && : \tau(z,t)=\tau_s(z)+\gamma(z)\exp(i\omega t)\\
&\text{Temperature} && : \theta(z,t)=\theta_s(z)+\delta(z)\exp(i\omega t)\\
&\text{Crystallinity} && : x(z,t)=x_s(z)+\phi(z)\exp(i\omega t)
\end{aligned} \tag{7}$$

where, ω represents frequency and $\alpha, \beta, \gamma, \delta, \phi$ the perturbed quantity of spinline area, velocity, stress, temperature, and crystallinity, respectively. Subscript s denotes a steady state.

Linearized governing equations could be made by introducing above perturbations in nonlinear governing equations (Eqs. (1)-(5)), as expressed below.

Complex linearized equation of continuity:

$$\alpha' = -\frac{v_s'}{v_s}\alpha + \frac{v_s'}{v_s^3}\beta - \frac{1}{v_s}\beta' - i\frac{\omega}{v_s}\alpha \tag{8}$$

Complex linearized equation of motion:

$$\beta' = \frac{1}{C_{in}v_s}\left[\begin{array}{l}(\tau_s v_s' + 0.905C_{ad}v_s^{3.095})\alpha + (\tau_s v_s)(\alpha')\\ +(-C_{in}v_s' - 1.19C_{ad}v_s^{1.095})\beta + \left(-\frac{v_s'}{v_s}\right)\gamma + (\gamma') - iC_{in}\omega\beta\end{array}\right] \tag{9}$$

Complex linearized constitutive equation (PTT model):

$$\gamma' = \frac{1}{v_s}\left[\begin{array}{l}(-\tau_s')\beta + \left(2(1-\xi)\tau_s + \frac{E_2}{De_0E_3}\right)\beta'\\ +\left(2(1-\xi)v_s' - \frac{E_1}{De_0E_3} - \frac{E_1 2\varepsilon\tau_s}{E_3\exp(3.2x_s)}\right)\gamma\\ +\left(\frac{E}{RT_0\theta_s^2}\left((v_s\tau_s' - 2(1-\xi)\tau_s v_s') - \frac{E_2 v_s'}{De_0E_3}\right)\right)\delta\\ +\left(\begin{array}{l}\frac{E_2\alpha^* v_s'}{De_0E_3} + \frac{6.4E_1\varepsilon\tau_s^2}{E_3\exp(3.2x_s)}\\ -(\alpha^* - 3.2)(v_s\tau_s' - 2(1-\xi)\tau_s v_s')\end{array}\right)\phi - i\omega\gamma\end{array}\right] \tag{10}$$

Complex linearized equation of energy:

$$\delta' = \frac{1}{v_s}\left[\begin{array}{l}\left(\frac{5}{6}Stv_s^{13/6}\psi^{1/6}(\theta_s - \theta_a)\right)\alpha\\ +\left(\begin{array}{l}\Delta H_f x_s' - \frac{1}{3}Stv_s^{1/6}\psi^{1/6}(\theta_s - \theta_a) - \theta_s'\\ +\frac{64}{3}Stv_s^{-11/6}\psi^{-5/6}v_y^2(\theta_s - \theta_a)\end{array}\right)\beta\\ +(-Stv_s^{7/6}\psi^{1/6})\delta + (\Delta H_f v_s)(\phi') - i\omega(\delta - \Delta H_f\phi)\end{array}\right] \tag{11}$$

Complex linearized crystallinity equation:

$$\phi' = \frac{1}{v_s}\left[\begin{array}{l}(-x_s')\beta + \left(E_4(1-x_s)(-8\ln 2)\left(\frac{\theta_s - \theta_a}{d^2}\right)\right)\delta\\ +(-E_4)\phi + (2E_4(1-x_s)\kappa De_0)\gamma - i\omega\phi\end{array}\right] \tag{12}$$

where,

$$E_1 = \exp\left(\frac{2\varepsilon De_0\tau_s}{\exp(3.2x_s)}\right),\quad E_2 = \exp\left[\frac{E}{RT_0}\left(\frac{1}{\theta_s} - 1\right) + \alpha^* x_s\right],$$

$$E_3 = \exp\left[\frac{E}{RT_0}\left(\frac{1}{\theta_s} - 1\right) + (\alpha^* - 3.2)x_s\right],$$

$$E_4 = k_m\exp\left[-4\ln 2\left(\frac{\theta_s - \theta_a}{d}\right)^2 + 2\kappa\tau_s De_0\right],$$

$$\psi = \left\{1 + 64\left(\frac{v_y}{v_s}\right)^2\right\},\quad (\,)' = \frac{\partial}{\partial z}$$

Perturbed variables, $\alpha, \beta, \gamma, \delta$, and ϕ have generally complex values. Eq. (13) indicates a possible perturbed input condition to be enforced in take-up velocity, spinneret area, extrusion velocity, or extrusion temperature.

$$\text{Take-up velocity: } \alpha(0)=\beta(0)=\delta(0)=\phi(0)=0,\ |\beta(1)|=1 \tag{13a}$$

$$\text{Spinneret area: } \beta(0)=\delta(0)=\phi(0)=\beta(1)=0,\ |\alpha(0)|=1 \tag{13b}$$

$$\text{Extrusion velocity: } \alpha(0)=\delta(0)=\phi(0)=\beta(1)=0,\ |\beta(0)|=1 \tag{13c}$$

Extrusion temperature: $\alpha(0)=\beta(0)=\phi(0)=\beta(1)=0, |\delta(0)|=1$ (13d)

By controlling the value of $\gamma(0)$ (i.e., both real and imaginary parts of γ), a perturbation of stress at spinneret, all state variables have been calculated by 4th-order Runge-Kutta method with shooting scheme, satisfying take-up boundary condition [8,18]. In this paper, take-up velocity and take-up area have been primarily adopted as an input and an output, respectively, based on the experimental method by Kikutani group [29].

SENSITIVITY RESULTS IN LOW-SPEED SPINNING

The effect of the degree of crystallinity formed in spinline on the sensitivity has been first analyzed for two different cases, as displayed in Fig. 2. All results of sensitivity show the resonant-like peaks along with the frequency, frequently encountered with hyperbolic system [30]. In comparison to the system without crystallization kinetics, the amplitude ratio (ratio of amplitudes between take-up area and an input disturbance) of take-up area with crystallization kinetics is lower under the partially developed crystallinity condition, implying the crystallinity makes the system less sensitive to disturbances in this case. This result coincided with the previous reports on the spinning sensitivity [21,22] under low degree of crystallinity and also showed similar trends in the stability one demonstrating that the crystallinity makes the system more stable from linear stability and nonlinear transient analyses [2].

Sensitivity of the system with crystallization kinetics has been further scrutinized by changing several key factors to affect the crystallinity state: drawdown ratio, relaxation time (or Deborah number), and FIC enhancement factor, κ. The effect of drawdown ratio on the sensitivity is depicted in Fig. 3. From the stability result (Fig. 3(a)), as drawdown ratio increases (the crystallinity also rises), the system becomes more stable at first and then less stable, finally unstable near maximum crystallinity (x=1). The sensitivity results have

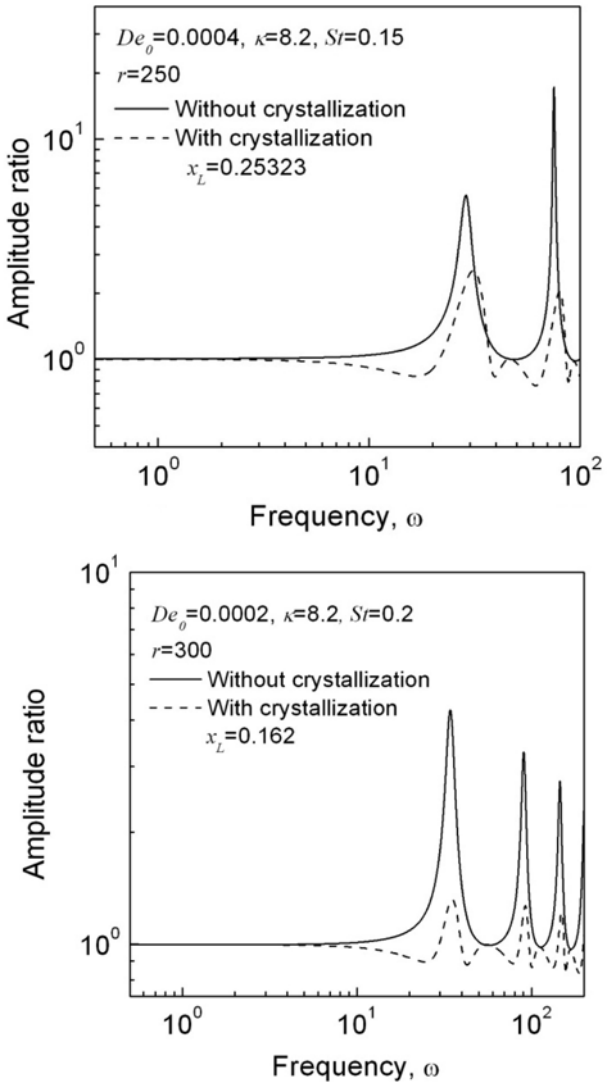

Fig. 2. Two examples showing amplitude ratios of spinline area at take-up along with frequency in low-speed spinning case when a disturbance is introduced at take-up velocity.

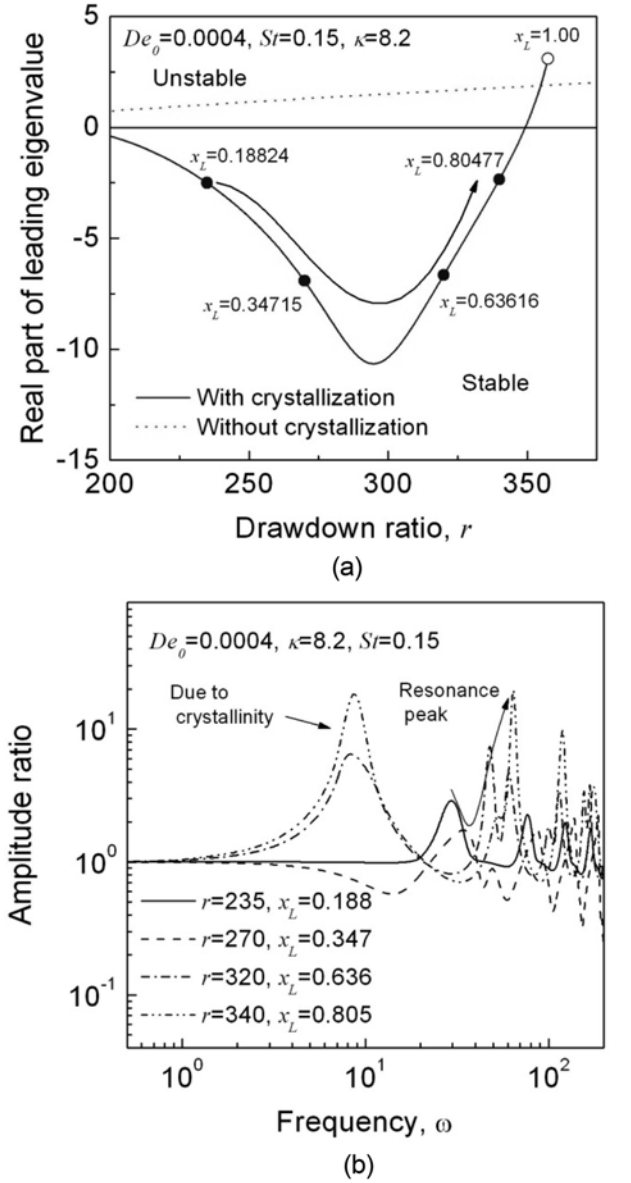

Fig. 3. Effect of drawdown ratio on (a) leading eigenmode and (b) frequency response in low-speed spinning process.

been compared between two sides based on maximum stable position (minimum real part of leading eigenvalue). In the left side, the system becomes less sensitive along with increasing drawdown ratio or the degree of crystallinity. Whereas, in the right side, the sensitivity of the system gradually gets larger, making the system more sensitive. It can be seen that the sensitivity results are remarkably different at two states with the same stable level (i.e., same leading eigenvalue) and as the crystallinity is being fully developed in the spinline, the resonant peaks are more pronounced. Moreover, the large resonance peak in low frequency regime is found as the crystallinity fully grows. Further studies will be required to shed light on such an interesting change of amplitude ratio in low frequency.

Above sensitivity results can be interpreted as the competition of effect of stabilizing crystallinity and destabilizing drawdown ratio. The existence of partially developed crystallinity makes the system more stable and less sensitive, but increasing drawdown ratio gives the opposite tendency. Under relatively low drawdown ratio conditions, the stabilizing effect of crystallinity might dominate the stability or sensitivity of the system, and then, when the drawdown ratio is further raised, the destabilizing effect of drawdown ratio compensate for the stabilizing effect of crystallinity. Moreover, as drawdown ratio rises after the crystallinity reaches its maximum, actual spinline distance available for deformation on the spinline is shortened [2], leading to more sensitive system. A similar explanation might be applied for the effects of the Deborah number and FIC enhancement factor, κ (Figs. 4 and 5). In other words, the low-speed spinning system with the crystallization kinetics is less sensitive under the conditions for low degree of crystallinity, but the system is getting more sensitive as the conditions are changed for enhancing crystallinity.

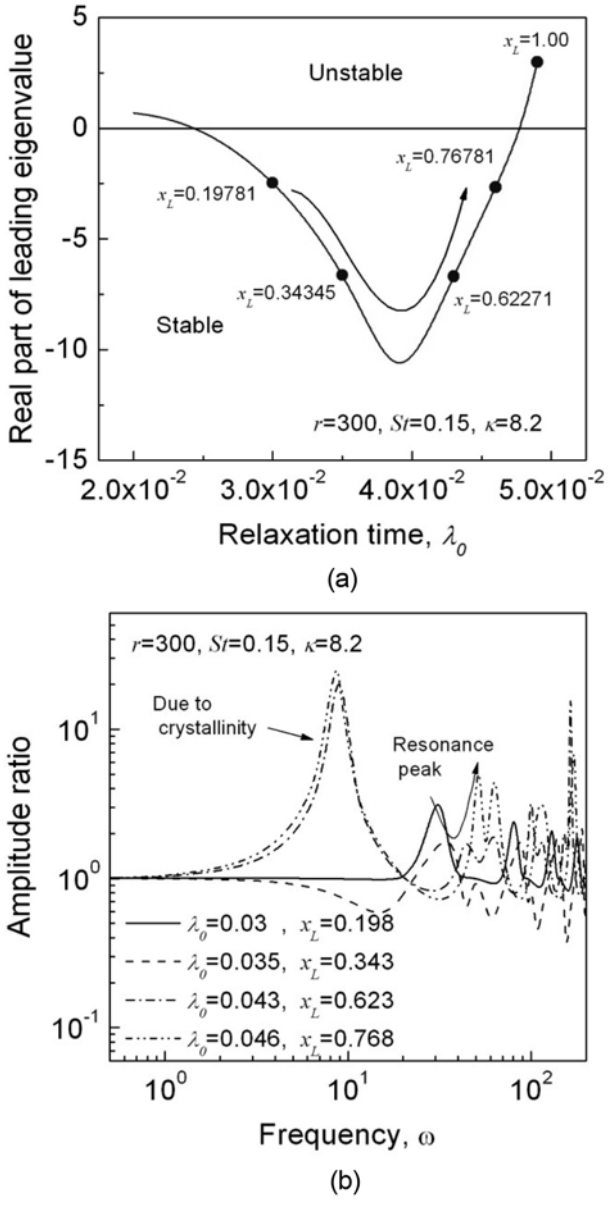

Fig. 4. Effect of relaxation time on (a) leading eigenmode and (b) frequency response in low-speed spinning process.

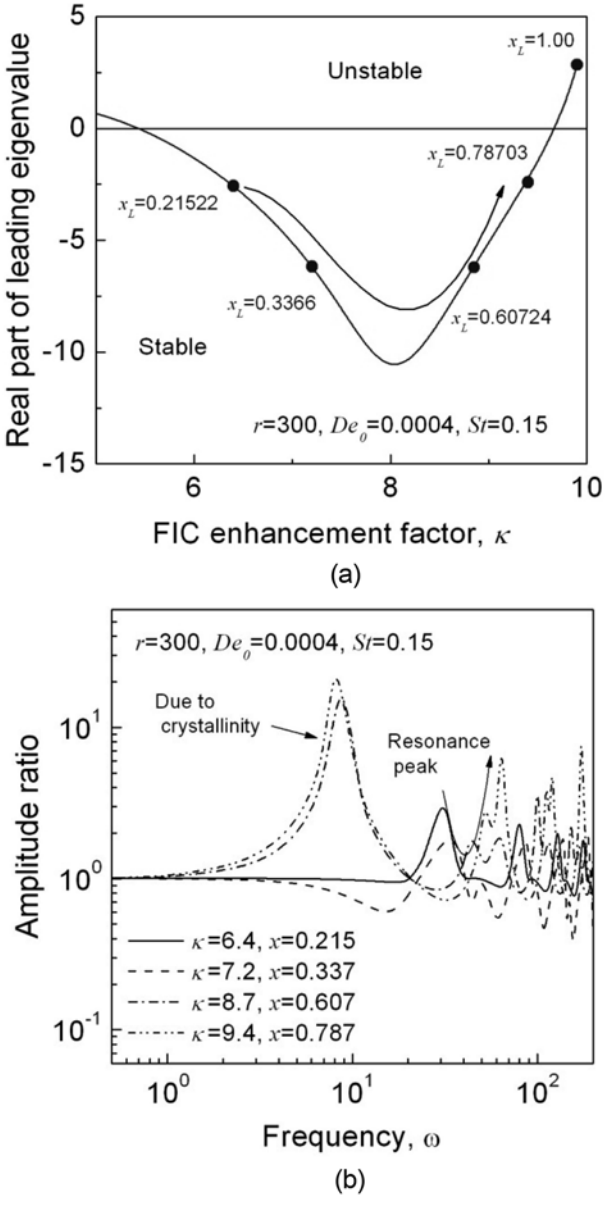

Fig. 5. Effect of FIC enhancement factor on (a) leading eigenmode and (b) frequency response in low-speed spinning process.

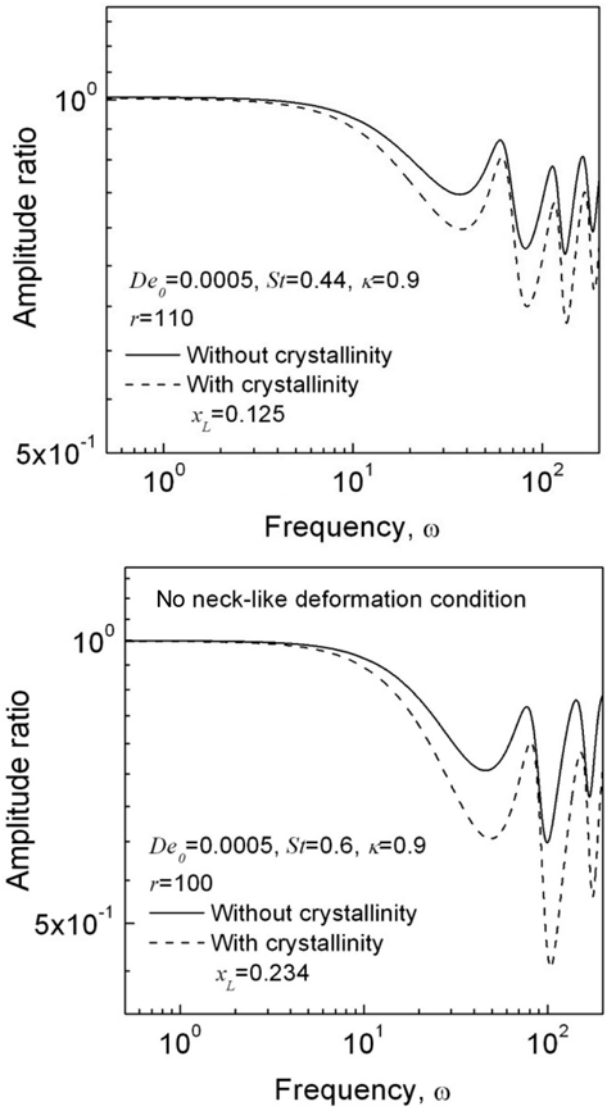

Fig. 6. Comparison of sensitivity results in two high-speed spinning cases with and without crystallinity.

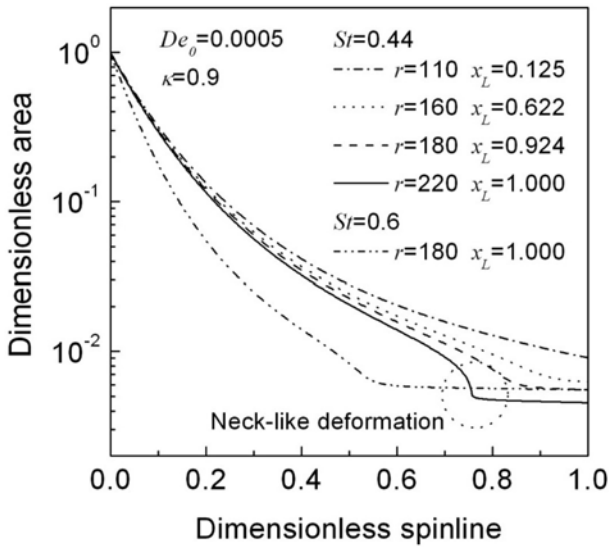

Fig. 7. Neck-like deformation in high-speed spinning process.

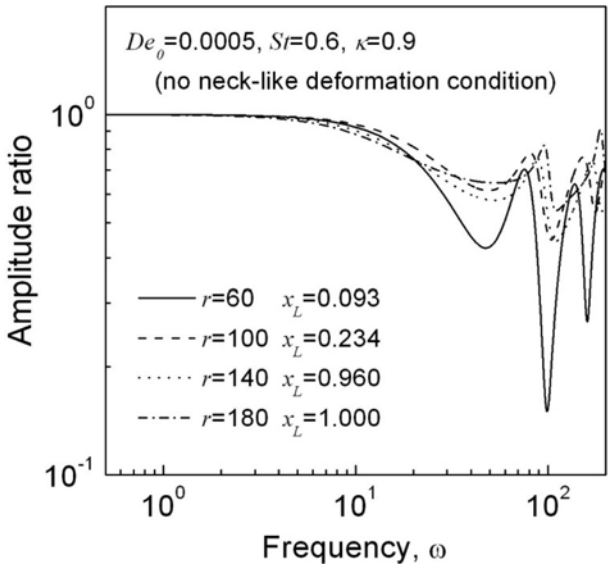

Fig. 8. Frequency response under the high-speed spinning conditions without neck-like deformation.

SENSITIVITY RESULTS IN HIGH-SPEED SPINNING

Fig. 6 exhibits two examples for the predicted amplitude of spinline area at take-up position along the frequency regime under the two high-speed conditions [3] when a sinusoidal disturbance is imposed at take-up velocity. In comparison with low-speed spinning case, the amplitudes generally have lower values than 1 due to the strong inertia force in spinline dynamics, stabilizing the system. The crystallinity not being fully developed makes the system less sensitive in these cases.

The neck-like deformation or necking occurring in high-speed spinning, which is featured by the abrupt reduction of spinline area where the crystallization in spinline is fully developed to its maximum (Fig. 7), is closely related to the change of extensional viscosity and appropriate spinline cooling [3]. This part focused on the effect of neck-like deformation on the sensitivity in the high-speed system. From previous published studies [3], it has been known that neck-like deformation stabilizes the system. In the case without neck-like deformation, the system becomes more sensitive as increasing drawdown ratio, corresponding with stability results [3] (Fig. 8) and sensitivity experiments [29]. However, the system becomes somewhat less sensitive at r=140 (x=0.960) just before the crystallinity is fully developed. It seems that in this drawdown ratio range from r=100 to r=140, the increasing degree of crystallinity slightly lowers the sensitivity of the system despite the destabilizing effect of drawdown ratio. Fig. 9 displays the amplitudes of take-up area when a perturbation is imposed at the take-up velocity or spinneret area under the condition for formation of necking. The sensitivity results in Fig. 9(a) are analogous with those of the system without neck-like deformation. However, after neck-like deformation occurs, r=220, the amplitude ratios of take-up area have the unity values, regardless of the frequency. This is because the ongoing perturbation is enforced after the location where the spinline

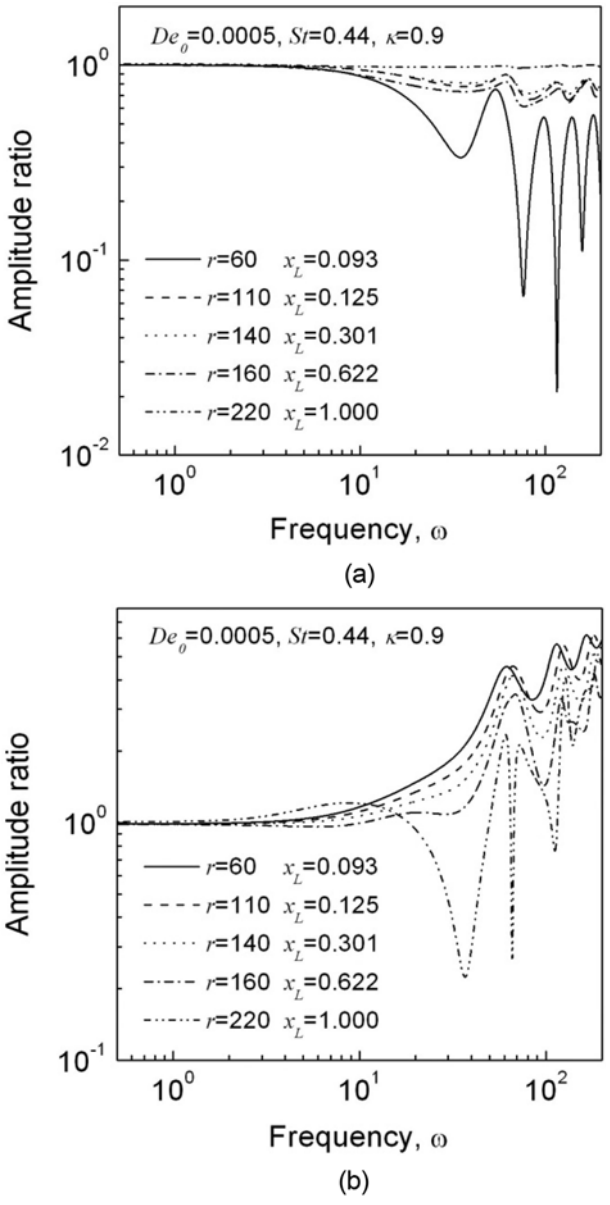

Fig. 9. Sensitivity results in the high-speed spinning case when a sinusoidal disturbance is imposed at (a) take-up velocity and (b) spinneret area, respectively.

area is tightly locked-in. Therefore, to clarify the effect of neck-like deformation on the sensitivity, another perturbation was introduced before the position where necking occurs, e.g., sinusoidal perturbation at spinline area. In this case, the neck-like deformation makes the system less sensitive, reducing the resonance peak level abruptly. It has been revealed that the sensitivity results quantitatively correspond with the stability results that neck-like deformation makes the system more stable in high-speed spinning process [3].

Briefly summarizing, the system becomes less sensitive under low crystallinity condition, and then becomes more sensitive with further increasing crystallinity or near maximum crystallinity. And, also the neck-like deformation in high-speed spinning case leads to less sensitive system or have unity response values, depending on the position in which the perturbation is imposed, e.g., before or after occurrence of the neck-like deformation. In both low- and high-speed spinning systems, the sensitivity results will provide important information on process development, supporting the stability results.

CONCLUSIONS

The effect of the flow-induced crystallization on the sensitivity in low- and high-speed spinning systems has been mainly examined using frequency response method. It turns out that the spinline crystallinity significantly affects the process sensitivity whether it is fully developed or not. The system is less sensitive to any disturbances under low level crystallinity formed in spinline but become more sensitive as the crystallinity is increasing. It has been confirmed here that such sensitivity trends in low-speed spinning case qualitatively coincide with those by stability analysis. It has been found that in the high-speed spinning system which is capable of producing neck-like deformation, the sensitivity results remarkably depend on the position of a sinusoidal disturbance. A conspicuous difference with the low-speed spinning case is that necking can make the system less sensitive even under the fully-developed crystallinity condition when a disturbance is introduced before necking in spinline. This theoretical methodology reported here will be effectively applied in other extensional deformation processes such as film casting and film blowing incorporated with crystallization kinetics.

ACKNOWLEDGMENTS

This study was supported by research grants from the Korea University and the Seoul R&BD program. Also, the support of the KOSEF (R01-2008-000-11701-0) is gratefully acknowledged.

NOMENCLATURE

a : dimensionless spinline area
A : dimensional spinline area
v : dimensionless spinline velocity
V : dimensional spinline velocity
t : dimensionless time
z : dimensionless spinline distance
L : dimensional spinline distance
r : drawdown
C_{in} : dimensionless inertia coefficient
C_{gr} : dimensionless gravity coefficient
C_{ad} : dimensionless air drag coefficient
g : coefficient of acceleration due to gravity
x : dimensionless crystallinity
De : Deborah number
St : stanton number
ΔH_f : dimensionless crystallization heat
C_p : heat capacity
T_{sp} : dimensional spinline temperature
X_∞ : maximum crystallinity
K_{max} : dimensional maximum crystallization rate
k_m : dimensionless maximum crystallization rate
T_{max} : dimensional maximum crystallization rate temperature
D : dimensional crystallization half width temperature rage

d : dimensionless crystallization half width temperature rage
τ : dimensional stress
η : fluid viscosity
ρ : fluid density
ε & ξ: Phan-Thien and Tanner model parameters
λ : fluid relaxation time
θ : dimensionless temperature
θ_m : dimensionless maximum crystallization rate temperature
ω : frequency
α : perturbed quantity of spinline area
β : perturbed quantity of spinline velocity
γ : perturbed quantity of spinline stress
δ : perturbed quantity of spinline temperature
ϕ : perturbed quantity of spinline crystallinity

Subscript
0 : die exit position
L : take-up position
a : cooling air condition

REFERENCES

1. J. S. Lee, D. M. Shin, H. W. Jung and J. C. Hyun, *J. Non-Newtonian Fluid Mech.*, **130**, 110 (2005).
2. D. M. Shin, J. S. Lee, H. W. Jung and J. C. Hyun, *Kor. Aust. Rheol. J.*, **17**, 63 (2005).
3. D. M. Shin, J. S. Lee, H. W. Jung and J. C. Hyun, *Rheol. Acta*, **45**, 575 (2006).
4. D. Gelder, *Ind. Eng. Chem. Fundam.*, **10**, 534 (1971).
5. R. J. Fisher and M. M. Denn, *AIChE J.*, **22**, 236 (1976).
6. M. M. Denn, Modeling for Process Control in *Advances in Control and Dynamic Systems*, *XV*, C. T. Leondes, Ed., Academic Press (1979).
7. S. Kase and M. Araki, *J. Appl. Polym. Sci.*, **27**, 4439 (1982).
8. B. M. Devereux and M. M. Denn, *Ind. Eng. Chem. Fundam.*, **33**, 2384 (1994).
9. W. W. Schultz, A. Zebib, S. H. Davis and Y. Lee, *J. Fluid Mech.*, **149**, 455 (1984).
10. A. K. Doufas and A. J. McHugh, *J. Non-Newtonian Fluid Mech.*, **92**, 81 (2000).
11. A. K. Doufas, A. J. McHugh and C. Miller, *J. Non-Newtonian Fluid Mech.*, **92**, 27 (2000).
12. Y. L. Joo, J. Sun, M. D. Smith, R. C. Armstrong, R. A. Brown and R. A. Ross, *J. Non-Newtonian Fluid Mech.*, **102**, 37 (2002).
13. H. W. Jung, H.-S. Song and J. C. Hyun, *J. Non-Newtonian Fluid Mech.*, **87**(2-3), 165 (1999).
14. H. W. Jung and J. C. Hyun, *Korean J. Chem. Eng.*, **16**(3), 325 (1999).
15. H. W. Jung, H.-S. Song and J. C. Hyun, *AIChE J.*, **46**, 2106 (2000).
16. J. S. Lee, H. W. Jung, S. H. Kim and J. C. Hyun, *J. Non-Newtonian Fluid Mech.*, **99**, 159 (2001).
17. H. W. Jung, J. S. Lee and J. C. Hyun, *Kor. Aust. Rheol. J.*, **14**, 57 (2002).
18. H. W. Jung, J. S. Lee, L. E. Scriven and J. C. Hyun, *Korean J. Chem. Eng.*, **21**, 20 (2004).
19. J. S. Lee, D. M. Shin, H. W. Jung, J. C. Hyun and Y. U. Jeong, *J. Soc. Rheol. Japan*, **33**, 2125 (2005).
20. J. H. Yun, D. M. Shin, J. S. Lee, H. W. Jung and J. C. Hyun, *J. Soc. Rheol. Japan*, **36**, 133 (2008).
21. W. H. Kohler and A. J. McHugh, *Chem. Eng. Sci.*, **62**, 2690 (2007).
22. W. H. Kohler and A. J. McHugh, *Polym. Eng. Sci.*, **48**, 88 (2008).
23. A. Ziabicki, *Fundamentals of fiber formation*, John Wiley and Sons (1976).
24. A. Ziabicki and H. Kawai, *High-speed fiber spinning: Science and engineering aspect*, John Wiley and Sons (1985).
25. N. Phan-Thien and R. I. Tanner, *J. Non-Newtonian Fluid Mech.*, **2**, 353 (1977).
26. I. A. Muslet and M. R. Kamal, *J. Rheol.*, **48**, 525 (2004).
27. R. Kolb, S. Seifert, N. Stribeck and H. G. Zachmann, *Polymer*, **41**, 1497 (2000).
28. H. Haberkorn, K. Hahn, H. Breuer, H. D. Dorrer and P. Matthies, *J. Appl. Polym. Sci.*, **47**, 1555 (1993).
29. W. Takarada, K. Kazama, H. Ito and T. Kikutani, *Intern. Polym. Proc.*, **19**, 380 (2004).
30. J. C. Friedly, *Dynamic behavior of processes*, Prentice-Hall, New Jersey (1972).
31. W. Minoshima, J. L. White and J. E. Spruiell, *Polym. Eng. Sci.*, **20**, 1166 (1980).
32. R. Zheng and P. K. Kennedy, *J. Rheol.*, **48**, 823 (2004).